Journal of Physics and Its Applications

Journal homepage: https://ejournal2.undip.ac.id/index.php/jpa/index



Analysis Of Dose Distribution Alpha and Secondary Particles in Therapy Alpha for Glioblastoma Cancer Using MCNP6 Software

Sheila Agustina^{1*}, Suharyana¹, Kusumandari¹, and Fajar Arianto²

¹Department of Physics, Sebelas Maret University, Surakarta, Central Java, Indonesia

*Corresponding author: asheila596@gmail.com suharyana61@staff.uns.ac.id kusumandari@staff.uns.ac.id fajararianto@fisika.fsm.undip.ac.id

ARTICLEINFO

Article history:

Received: 3 February 2025 Accepted: 9 October 2025

Available online: 27 November 2025

Keywords: MCNP6 α Therapy Glioblastoma Brain Cancer Secondary Particles

ABSTRACT

The α therapy modeling was performed for the treatment of glioblastoma brain cancer using MCNP6 software. The simulation used a head and neck phantom geometry, with a spherical shape of the radiation direction of the cancer cells with a radius of one cm divided into 27 targets. One radiation source is directed to each target center of the cancer cells with five energy variations, namely (430, 425, 415, 410, and 400) MeV. The simulation results are in the form of a distribution of absorbed doses in all targets and healthy cells around them. The simulation results show an average dose distribution of (1.2902 \pm 0.0024) 10^{-11} Gy/ α with an isodose level of 69.75%. The healthy organ that receives the largest dose and secondary particle distribution after cancer cells is the brain, with an accumulative dose of (1.7446 \pm 0.0033) 10^{-15} Gy/ α . The dose distribution on cancer cells shows that the irradiation time to kill glioblastoma cancer cells is (1456 \pm 0.14) seconds with an α current of 1 nA.

1. Introduction

Glioblastoma, or scientifically known as glioma cerebri, is a type of cancer located in the center of the brain and is formed from abnormal tissue that grows from cells that make up brain tissue. Glioblastoma cancer is not like other types of cancer that are in the form of lumps; this cancer is in the form of cancer threads that can spread quickly and can infiltrate the brain tissue and its surroundings, even simultaneously [1]. Glioblastoma is known to be very malignant, where the development of its cells is included in the category of aggressive development. There is necrosis or dead cells, and its development is very rapid without any previous lesions. Based on the results of the survival rate, this cancer is estimated to grow approximately 12 months after being diagnosed [2].

Glioblastomas typically develop in the frontal and lateral brain regions. These areas play a key role in cognitive function, emotion, and sensory processing. They can also occur in the brainstem and spinal cord, although this is less common. The cancer target studied by Jiang et al. (2021) measured 2 cm in diameter, as shown in Fig. 1 [3].

In the process of treating patients suffering from brain cancer, there are several treatment methods, including oncological surgery, chemotherapy, and radiotherapy. In the case of patients suffering from glioblastoma cancer cells, surgical removal of cancer cells is sometimes ineffective, because the ability of glioblastoma to spread easily allows tumor tissue to remain in the brain even after surgery [4].

Furthermore, performing a surgical procedure has more serious consequences, where this procedure is difficult and dangerous to perform. This is because it can cause recurrence after surgery. Glioblastoma cancer grows and develops in the cerebrum (center of the brain), specifically in the frontal lobe (front of the brain) and in the temporal lobe (side of the brain) [5]. The location of glioblastoma cancer in the cerebrum and deep within the brain parenchyma makes surgical procedures difficult.

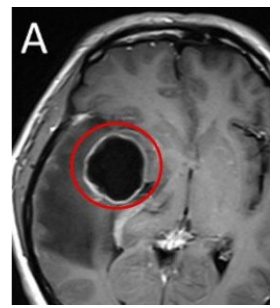


Fig. 1: MRI results of glioblastoma cancer.

²Department of Physics, Universitas Diponegoro, Jl. Prof. Sudarto, SH, Tembalang, Semarang, Indonesia 50275

Radiation therapy, or radiotherapy (RT), is one of the modalities in treating cancer by utilizing high-energy ionizing radiation, where this radiation will be used to kill and stop the division process of cancer cells by focusing it on cancer cells [6]. Radiotherapy has advantages over other techniques because it focuses on cancer cells and maintains healthy cells in the area around the cancer cells to continue to function properly. Radiotherapy is one of the methods chosen in the treatment of brain cancer. In radiotherapy, radiation will be aimed at damaging the DNA molecules of cancer cells, with the aim of changing the DNA of cancer cells and stopping their development. Based on this event, there are direct and indirect ionization effects.

The α therapy is a type of radiotherapy that kills cancer cells by utilizing α energy, which began to be developed in clinical trials in 1975 at Lawrence Berkeley National Laboratory (LBNL) and has treated more than 700 patients [7]. The α therapy has advantages, including being able to maximize the dose that goes to cancer cells, minimize the dose received by healthy tissue around cancer cells, and the dose given by α therapy can reach deep cancer cell positions [8].

 α particles are the most effective particles for killing cells, because they have the most effective ionization power of 20 compared to other particles such as protons, electrons, or photons. This causes α particles to have a very high level of damage to a material that passes through such as cancer cells. α particles have a higher mass compared to the mass of other particles, namely $4.00152\times10^{-27}~\mu m$ and have a very short range.

α therapy also has a characteristic called the Bragg peak in its dose distribution. This Bragg curve is a characteristic dose curve resulting from the dose deposition process of a radiation particle. When the α particle penetrates a material, the α particle will move slower. The slow movement of the α particle as a function of depth. As a result of the decreasing speed of the α particle, it will cause an increase in the level of energy loss. This rate of energy loss is often referred to as Linear Energy Transfer (LET). The process that occurs is called dose deposition, where the process continues until all the energy of the α particles is used up. After the energy of the α particles is used up, this process will stop suddenly [9]. α particles have a higher LET value of 100-2000 keV/um when compared to other radiation particles because α particles are included in the heavy ion category [10].

Based on Fig. 2, it shows that α particles have a sharper Bragg peak decrease compared to protons and photons. If applied in therapy, α particles have a lower risk of hitting healthy cells behind healthy cells. In addition, compared to carbon ions, α particles experience fewer nuclear fragmentation processes, resulting in better distal dose conformity due to reduced "fragmentation tails". The less complex secondary fragment spectrum also reduces uncertainty in estimating biological effects compared to carbon ions. In addition, α particles also have higher LET values when compared to carbon ion LET.

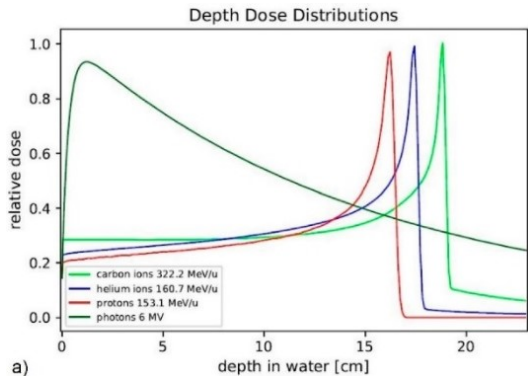


Fig. 2: Bragg peaks of α particles compared to photons, protons, and carbon [11].

Currently, the use of α particles for clinical treatment has been carried out at the Heidelberg Ion Therapy Center (HIT) [12]. In cancer treatment, using α particles will show a lower range compared to other particle beams, so it will produce a sharper Bragg peak [12].

Radiation dosimetry is a method used to calculate the amount of radiation energy stored in a material through direct or indirect ionization processes. Radiation dose is the amount of radiation energy stored (absorbed) into a material that has been passed through or the amount of exposure to radiation. Radiation dose can be measured by a method called radiation dosimetry. In the absorbed dose, several units are used: exposure and absorbed dose. Exposure is defined as the ability of ionizing radiation to activate ionization in the air through which X-ray and radiation passes in a certain volume. The absorbed dose represents the average energy (dE) absorbed in something passed by radiation particles in unit mass (dm), written with Eq. 1 [13]:

$$D = \frac{dE}{dm} \tag{1}$$

Absorbed dose is used to assess the potential for biochemical changes in certain tissues. The units of absorbed dose are Joule/kg or Gray (Gy) [13].

Three main interactions of α particles with atoms are ionization, excitation, and inelastic nuclear interactions. Three interactions of α particles with atoms, one of the interactions that will produce a Bragg curve that describes the characteristics of α particles and describes the distribution of absorbed doses in body tissues. The interaction is the ionization process, where this interaction dominates [14]. The dominant interaction is ionization (Fig. 1) with atomic electrons. This interaction is important because it releases atomic electrons that create anesthetics that kill cancer cells [9]. The α particles will continue to lose energy when they collide with atoms of matter that are passed during the ionization process.

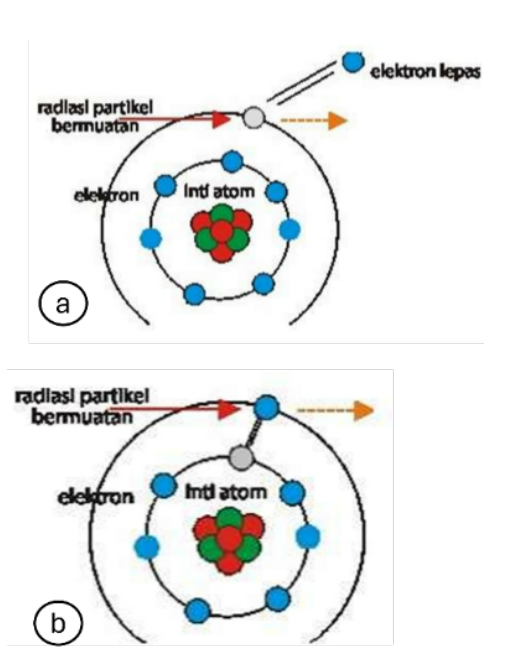


Fig. 3: Interaction of α particles with atoms: (a) ionization, (b) excitation.

Many efforts have been made to improve the accuracy of calculations for radiotherapy, one of which is by using the Monte Carlo method, which has the highest level of accuracy. Simulation using Monte Carlo is a statistical method whereby, using this method, it can trace the initial journey of particles until the particles disappear. The software used in this Monte Carlo simulation is Monte Carlo N-Particle (MCNP), which is useful in numerical calculations with analysis [15]. The Bragg peaks on all partitions in cancer cells are analyzed to obtain isodose results, which can utilize the Monte Carlo method. Monte Carlo is a technique that is widely used in planning proton therapy optimization. Computing power allows simulations to be carried out to plan proton therapy treatments with pencil beams. This method looks for the probability that occurs between interactions with the distribution of protons in a material that is passed through. The amount of energy required, and the range (depth) required in the radiation process can be determined [16]. Simulation with Monte Carlo obtains information about the absorbed dose in patients with glioblastoma cancer.

Based on previous research conducted by [17], the study was conducted with a simulation using a pencil beam collimator for proton beam irradiation. In this study, MCNP6.2 software was used to create proton therapy using a 3×3×3 pencil beam scanning Rubik's cube for glioblastoma cancer using MCNP6. The irradiation area for glioblastoma cancer cells was modeled with a geometric shape, namely a cubic using a side size of 1.2 cm which was divided into 27 small cubicles using a side size of 0.4 cm. The proton beam used energies of 105, 108 and 111 MeV from the left side of the phantom and a beam diameter of 0.05 cm directed to each center of the 27 cubicles of the cube. However, this study has not considered the relative dose difference in each cubicle of cancer cells to obtain the isodose level, has not considered the dose for each secondary particle that appears in healthy organs around the cancer cells, and the length of time used during irradiation has not been considered.

Furthermore, the research was continued by Wardani (2023), this study used MCNP6.2 software with proton therapy using a 3×3×3 pencil beam scanning rubik for glioblastoma cancer. The irradiation area for glioblastoma cancer cells was modeled with a geometric shape, namely a cube divided into 27 small cubicles using a side size of 0.4 cm. The proton beam used energies of 113; 112.9; 108.5 MeV. In this study, the MCNP feature was developed to obtain information about secondary particles in healthy organs around cancer cells, calculations related to the length of irradiation time used for therapy on glioblastoma cancer cells, and the acquisition of isodose levels that can be seen from the relative difference in each part of the glioblastoma cancer cell cubicle. The result was a successful proton dose distribution. The healthy organ that received the largest proton dose distribution and secondary particles was the brain. The results of the simulation using the MCNP proton therapy software obtained an even dose distribution in each cubicle of cancer cells, with an average dose value of (1.400 ± 0.005) MeV/g per proton and an isodose value of 94%. However, in this study, cancer cells were modeled with a geometric shape, namely a cube, cancer cells have an abstract shape.

The research written this time updates the research conducted by Maharani (2022) and Wardani (2023) by replacing the therapy particle with α particles. In this study, a simulation of α therapy was carried out using Monte Carlo N-Particle software with a geometric shape of the radiation target, namely a sphere divided into 27 targets, this is based on the abstract shape of cancer cells and to be more varied. In this study, an energy range of 400 MeV-430 MeV was used. To simulate α beam radiation, pencil beam scanning was used. In addition, the MCNP feature was further developed to obtain information about secondary particles in healthy organs around cancer cells. Then, the length of radiation time used for therapy on glioblastoma brain cancer was calculated. The phantom that will be used is a phantom of the head and neck. Therefore, in this study, it is attempted that all cancer target cells can obtain dose results, or no targets have a dose value of 0. In addition, it can calculate the absorbed dose received by healthy organs around cancer cells due to secondary particles and calculate the total irradiation time required.

2. Methods

This study used Monte Carlo simulations with MCNP6 software. MCNP6 was chosen for its ability to accurately model particle transport in complex geometries and its established use in radiation therapy planning. Phantom will be used as a reference in creating MIRD phantom geometry. This study used phantoms of the head and neck, then augmented with the geometry of the PBS (Pencil Beam Scanning) irradiation area for glioblastoma cancer cells. The phantom was created in accordance with the ORNL-MIRD (Oak Ridge National Laboratory - Medical Internal Radiation Dose) phantom standard. The dose distribution in the PBS irradiation area and surrounding healthy cells was then calculated with varying energies (430, 425, 415, 410, and 400) MeV. The output was then calculated as the deposited energy in MeV/gram per α , which

was then represented graphically, showing the Bragg peak.

This study used one α radiation source placed parallel to the forehead. The source location was chosen based on the "As Low As Reasonably Achievable" (ALARA) principle.

Anatomically, glioblastoma cancer cells grow in the cerebrum (the center of the brain), specifically in the frontal lobe. Therefore, the most appropriate direction for radiation is in front of the forehead, which maximizes the α dose reaching cancer cells and minimizes the α dose reaching healthy cells.

3. Result and Discussion

The phantom geometry model used is the head and neck phantom, which is made with the ORNL-MIRD (Oak Ridge National Laboratory - Medical Internal Radiation Dose) phantom standard by adding the target geometry of the irradiation area for glioblastoma cancer cells. The geometry of this irradiation area is modeled in the form of a sphere with a radius of 1 cm, which is divided into 27 partitions. Figure 4 shows the geometry of the phantom, and the irradiation area created.

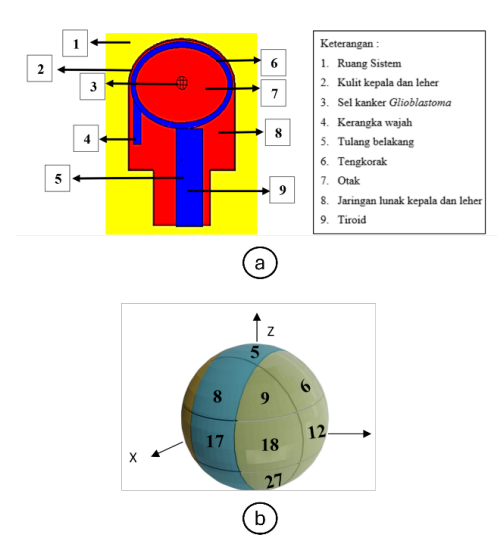


Fig. 4: (a) Geometry of the head and neck phantom, (b) Magnification of the direction of radiation geometry of glioblastoma cancer cells.

Figure 4(a) shows the geometry of a head and neck phantom. The densities used in the phantom are soft tissue, bone, and void space. The differences in density can be seen in the color scheme in Fig. 4(a): yellow is used for void space density, blue is used for bone density, and red is used for soft tissue density.

After the head and neck phantoms were created, the Pencil Beam Scanning (PBS) radiation area geometry for glioblastoma cancer cells was added. Figure 4(b) shows the radiation direction geometry of the cancer cells. This radiation area geometry was modeled as a sphere with a radius of 1 cm. The rationale for using the spherical geometry and its size is based on the results of a cancer MRI study by Jiang et al., 2021, which had a radius of 1 cm from the glioblastoma MRI scan, as shown in Fig. 1. The geometry was then divided into 27 targets, each measuring 0.33 cm in length. The geometry was divided into 27 partitions to assess isodose levels. The partition division seen from the X, Y, and Z positions is shown in Fig. 5 below:

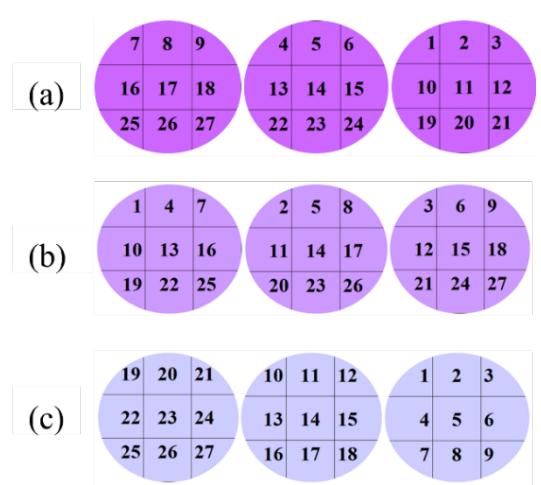


Fig. 5: Target cell numbers are seen on each axis: (a) Target number on the X axis (seen from the front of the body), (b) Target number on the Y axis (seen from the right side of the body), (c) Target number on the Z axis (seen from the top of the body).

Figure 5 (a) shows a slice of the sphere cutting the x-axis from the front of the body with the positions in order from left being the closest part to the middle part-farthest part from the source. Figure 5 (b) shows a slice cutting the y-axis from the right of the body with the positions in order from left being the front-middle part-back part. Figure 5 (c) shows a slice cutting the z-axis from the top of the body with the positions in order from left being the top-middle part-bottom part.

Optimization of the number of particle histories α is carried out with the aim of determining the number of repetitions carried out in the simulation process. The more repetitions carried out in the simulation process, the smaller the relative error value (KR) produced, but this affects the running time, which is getting longer. Therefore, it is necessary to determine the NPS optimization to obtain acceptable results but with a running time that is not too long. The simulation of the optimization of the number of particle histories was carried out with an NPS of 177,500. The results of this running are in the form of relative error values and Variance of Variance (VOV), which are used to estimate the error variance of the relative error. The simulation output is then visualized in the form of a graph as shown in Fig. 6 and Fig. 7:

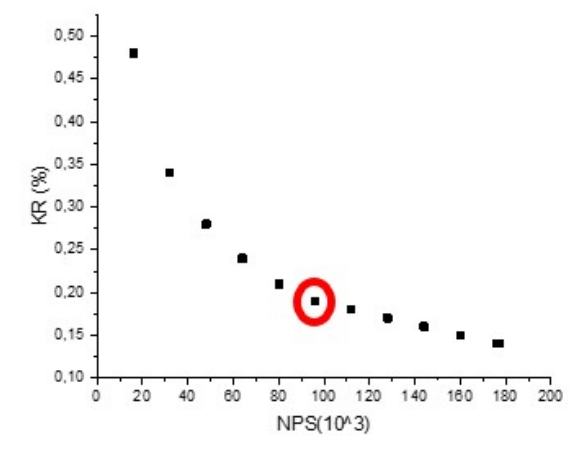


Fig. 6: Graph of the relationship between NPS and relative error.

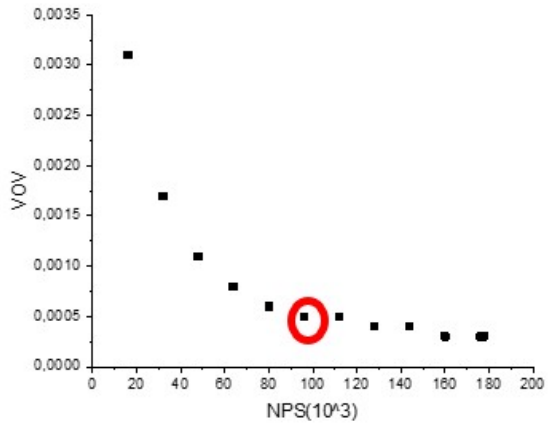


Fig. 7: Graph of the relationship between NPS and relative errors.

A comparison graph is obtained between the relative error value and VOV, NPS. The optimal NPS value is 96×103 chosen based on the results of the analysis of the two indicators because the value has a VOV value <0.1, which is 0.0005, and a KR value of 0.19% in accordance with the requirement that the relative error value is <0.1 or 10%.

In this study, a simulation of α particle irradiation was carried out from the left as far as 25 cm towards the target of spherical cancer cells, which were partitioned into 27 partitions with a length of each side of 0.33 cm. This research simulation was carried out using pencil beam scanning of 0.33 cm. This irradiation was carried out to see the distribution of dose distribution on tumor cells and the distribution of dose distribution that affects healthy organs.

Before conducting the therapy simulation, the location of the α particle source was defined. The center of the cancer cells is in the brain, with the center of the cancer 5.4 cm from the skin surface. Therefore, the α source was chosen to be 25 cm from the center of the cancer cells, or 19.6 cm from the skin surface. The α source position, 25 cm from the center of the cancer cells, was chosen because this position refers to an ideal gantry [17].

In this study, the α radiation source was placed 25 cm from the center of the cancer cells. The pencil beam collimator used for irradiation had a diameter of 0.33 cm, corresponding to the size of the 27 partitions. The α beam was then directed to each partition center. This irradiation was carried out to determine the dose distribution to the cancer cells to obtain isodose values, as well as the distribution of the dose to healthy organs. Figure 8 shows the location of the proton source relative to the cancer cells. The selection of the source location is based on the ALARA principle, considering healthy organs around the cancer cells such as the cerebellum, spine, facial skeleton, and eyes so that they are not exposed to radiation from the α source. The location of the α particle source is shown in Fig. 8.

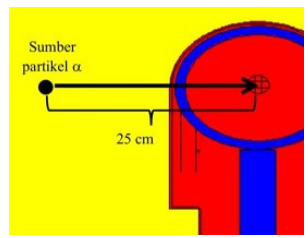


Fig. 8: Illustration of the location of the α source in relation to cancer cells in the phantom.

After defining the source, the next step is to determine the energy to be used for the simulation. The determination of the α particle energy is done with the aim of providing optimal dose distribution to target cells and maximizing the effectiveness of radiation therapy in accordance with the ALARA principle. The energy range is determined by selecting the maximum and minimum energy that can reach cancer cells. The maximum energy is determined by selecting the α particle energy, then irradiating with the selected energy and observing whether the energy used can reach the cancer cell partition farthest from the radiation source. To determine the minimum energy is also done by selecting the α particle energy, then irradiating with the selected energy and observing whether the energy used can reach the cancer cell partition closest to the radiation source. In this study, the maximum energy was chosen at 430 MeV and the minimum energy at 390 MeV based on the results of the particle track plot during the irradiation process visualized in Fig. 9.

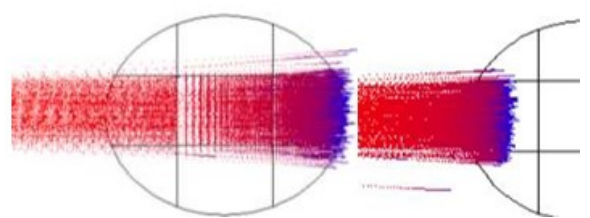


Fig. 9: (a) shows that with an energy of 430 MeV, the α particle can reach the partition furthest from the source. (b) shows that with an energy of 390 MeV, the α particle can reach the partition closest to the α source.

Energy determination is done after defining the source used for simulation. Determination of particle energy α is done with the aim of providing optimal dose distribution to target cells and maximizing the effectiveness of radiation therapy in accordance with the ALARA principle. Energy determination is initially done by looking at the results of the track plot on the vise. The minimum energy used in the study was 400 MeV, and the maximum energy used was 430 MeV. After obtaining the minimum and maximum energy, running was carried out until the results were obtained in the form of depth and dose values, and then a Bragg peak graph was made as in Fig. 10.

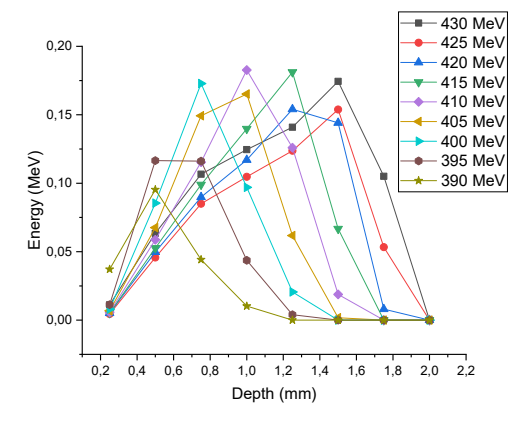


Fig. 10: Graph of deposited energy at the depth point of the α particle trajectory in the energy range 400 – 430 MeV.

Determination of the energy range of this energy is done by using variations of nine energies, starting from a minimum energy of 400 MeV to a maximum energy of 430 MeV so that a graph is obtained as in Fig. 7. Based on the results of the Bragg peak graph in Fig. 8, the effective energy for the α therapy simulation is at energies of 400, 410, 415, 425, and 430 MeV. This is because the five energies can reach the deepest cells. The reason for choosing the minimum energy used of 400 MeV is because it is based on Fig. 7. The Bragg peaks at energies of 390 MeV and 395 MeV have lower Bragg peaks compared to the 400 MeV energy.

The energy range is to be used for simulation; the next process is running. The results of running the program obtained an accumulative dose that is evenly distributed to all partitions in the tumor cells. Partitions near the source receive doses from energies of 400 MeV and 410 MeV. The middle partition receives doses from energies of 410 MeV, 415 MeV, and 425 MeV. The back partition receives doses from energies of 415 MeV, 425 MeV, and 430 MeV. The accumulative dose of 27 partitions is as shown on Fig. 11.

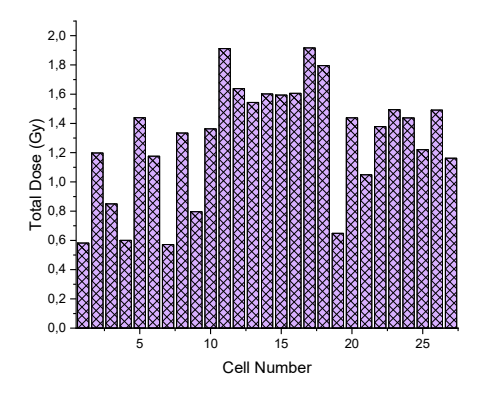
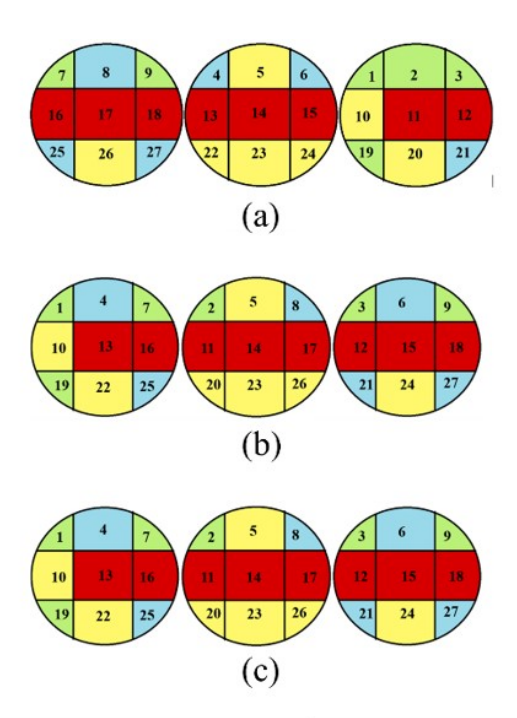


Fig. 11: Accumulative dose diagram on 27 cancer cell targets.

Figure 11 shows the results of the accumulated radiation dose on 27 cell targets. The calculation results produce a dose value with a range between $(0.57 - 1.92) \times 10-11$ Gy/ α with an accumulative dose of all cancer cell targets of $(3.48 \pm 0.006) \times 10-11$ Gy/α and an average dose of (1.29 ± 0.01) × 10-11 Gy/α , and a KR of 30.25%. As for the data obtained, they are listed in Appendix 5. According to research conducted by Liu et al. (2019), the KR value is <20%, but in this study the accumulated dose received by 27 cell targets with combined energies of 430 MeV, 425 MeV, 415 MeV, 410 MeV, and 400 MeV showed an isodose result of 69.75% [17]. Differences in dose values can be caused by various factors, including the geometric shape of the target cell size, which is not the same, resulting in differences in volume size; the size of the pencil beam, which causes side effects on the widening of the beam, which can be stacked [18]; less varied energy and intensity; and the number of target cells is not large enough.

The results of the dose distribution on tumor cells are then visualized through the dose contour from 3 sides, namely the X axis, Y axis, and Z axis. This dose distribution visualization is carried out to provide information on the distribution of doses in the target area by showing partitions that receive high or low doses.



Range Dosis (Gy/α)	Warna
$(0,50-1,00) \times 10^{-11}$	
$(1,01-1,35) \times 10^{-11}$	
$(1,36-1,50) \times 10^{-11}$	
>1,51 × 10 ⁻¹¹	

Fig. 12: Z Visualization of the dose distribution 2 on (a) X axis, (b) Y axis, (c) Z axis.

Figure 12 shows the visualization of the dose distribution in each partition as seen from the X, Y, and Z axes. There are different colors in each cell partition, this indicates the dose range received by the target cells. The dose distribution in green shows the first lowest dose received by cancer cells of $(0.50-1.00) \times 10^{-11}$ Gy/ α . The blue color shows the second lowest dose received by cancer cells of (1.01-1.35) $\times 10^{-11}$ Gy/ α . The yellow color shows the middle dose distribution received by cancer cells of $(1.36-1.50) \times 10^{-11}$ Gy/ α . The red color shows the highest dose received by cancer cells of >1.51 $\times 10^{-11}$ Gy/α . Based on the contour graph, it is known that the largest dose α is in the middle partition, this is because the middle partition receives an additional dose from the scattered dose fired to the sides. Therefore, the dose received by the middle partition is greater.

The treatment of radiation exposure of α particles to cancer cells in the brain does not rule out the possibility that radiation rays will be scattered out of the cancer cells. Healthy cells that are passed by $\boldsymbol{\alpha}$ particles will also be exposed to radiation doses; therefore, the dose that hits healthy cells needs to be calculated so that α particle therapy remains in accordance with the ALARA principle. The possibility of a dose of α particles scattered out of cancer cells also needs to be calculated because it affects the effectiveness of α therapy in killing cancer cells. The α particles that interact with material will produce secondary particles that have the potential to cause secondary cancer, so the presence of these secondary particles also needs to be calculated. Healthy cells that are expected to receive α scattered doses and doses from secondary particles are the brain, skull, facial skeleton, spine, soft tissue, and

skin. The secondary dose received by healthy cells needs to be calculated so that healthy cells are still within the safe OAR limit, as shown in Table 1.

The second largest dose after cancer cells is in the brain organ that receives a dose of α , which is (1.74 ± 0.01) x 10^{-15} Gy (Fig. 12). The brain organ is an organ that is directly passed through during irradiation, as well as tumor cells located in the brain organ. The results of the α scatter dose distribution obtained are still far below the Organ At Risk (OAR) tolerance limit. The brain organ with the largest scatter dose receives 0.015% of the dose received by tumor cells (Table 1).

Table 1: The quantities of the k-fitting

Table 1: The quantities of the k-fitting.		
Organ	Accumulative Dose (Gy/α)	Relative to Cancer Cells
	α	(%)
Cancer Cells	(1.29±0.01) x10 ⁻	-
Brain	(1.74±0.01) x10 ⁻	0.015
Skull	(1.62±0.01) x10 ⁻	0.013
Facial Skeleton	(1.55±0.01) x10 ⁻	0.011
Spine	(0.92±0.01) x10 ⁻	0.007
Soft tissue of the head and neck	(1.42±0.01) x10 ⁻	0.010
Skin	(1.55±0.01) x10 ⁻	0.012

Table 2: Duration of irradiation for each energy.

Table 2. Duration of irradiation for each energy.			
Exposure	Energy (MeV)	Exposure Time (s)	
1	430	625.17	
2	425	625.99	
3	415	672.88	
4	410	580.75	
5	400	408.00	
Amount		2912.79	
	,		

The duration of radiation exposure is crucial in α therapy because it affects the dose received by the patient. The Treatment Planning System (TPS) ensures that cancer cells receive the prescribed dose and are administered in the shortest possible time. The goal of planning the duration of radiation exposure is to minimize the risk of radiation side effects, which aligns with radiation protection measures (ALARA). According to research conducted by Wardhani (2023), an accumulative dose of 52 Gy is required to kill glioblastoma brain cancer cells. This study used an α current of 1 nA. The α current is related to the amount of simulated α . The resulting dose from the simulation was then used as the highest accumulative dose to the cancer cells, which is (5.72 ± 0.01) 10^{-12} Gy/ α . This is because the maximum dose is required to kill all cancer cells. The calculation results then obtained the irradiation time for each energy, as shown in Table 2. The total irradiation time for glioblastoma cancer cells was (2912.79 ± 0.009) seconds. The purpose of calculating the irradiation time for each energy was to provide an idea of the time required to kill cancer cells with a given energy level.

4. Conclusion

The simulation of α therapy for glioblastoma cancer cells from the left can be done using 5 energy variations, namely at 400 MeV, 410 MeV, 415 MeV, 425 MeV, and 430 MeV. The dose distribution in glioblastoma cancer cells is (1.29 \pm 0.01) 10-11 Gy / α and an isodose level of 69.75%. Six healthy organs around the cancer cells receiving a scatter dose from α particles and a scatter dose of secondary particles. The healthy organ that received the second largest dose was the brain (1.74 \pm 0.01)10-15 Gy / α Gy. The dose was within safe limits of OAR; the ratio of healthy cell doses to tumor cells was 0.015%. The total therapy time required for therapy of craniopharyngioma tumor with a lethal dose of 52 Gy and a current of 1 nA (2912.79 \pm 0.009) seconds.

Acknowledgment

Thanks to the supervisor who has helped the author during the research and Mr. Dr. Azizul Khakhim who has lent the author the MCNP6 software.

References

- [1] A. Broniscer, O. Chamdine, S. Hwang, T. Lin, S. Pounds, A. O. Thomas, S. Shurtleff, S. Allen, A. Gajjar, P. Northcott, and B. A. Orr, "Gliomatosis Cerebri in Children Shares Molecular Characteristics with other Pediatric Gliomas" Acta Neuropathol., 131, 299–307, (2016).
- [2] S. Archontidi, S. Joppé, Y. Khenniche, C. Bardella, and E. Huillard, "Mouse Models of Diffuse Lower-Grade Gliomas of the Adult" in Brain Tumors, G. Seano, Ed. Springer, 3–38, (2021).
- [3] H. Jiang, K. Yu, Y. Cui, X. Ren, and S. Lin, "Differential predictors and clinical implications associated with long-term survivors in idh wildtype and mutant glioblastoma" Front. Oncol., 11, 2–3, (2021).
- [4] S. Nurwati and R. I. Prasetya, "Kajian Medis Pemanfaatan Teknologi Nuklir BNCT untuk Tumor Otak Jenis Glioma" in Prosiding Pertemuan dan Presentasi Ilmiah, 127–134, (2014).
- [5] C. C. Ko, M. Hong, C. F. Li, T. Y. Chen, J. H. Chen, G. Shu, Y. T. Kuo, and Y. C. Lee, "Differentiation between Glioblastoma Multiforme and Primary Cerebral Lymphoma: Additional Benefits of Quantitative Diffusion Weighted MR Imaging" PLoS One, 11(9), 1–15, (2016).
- [6] N. J. DeNunzio and T. I. Yock, "Modern Radiotherapy for Pediatric Brain Tumors" Cancers, 12(1), 1533, (2020).
- [7] A. Mairani, S. Mein, E. Blakely, J. Debus, M. Durante, A. Ferrari, H. Fuchs, and D. Georg, "Roadmap: Helium Ion Therapy" Phys. Med. Biol., 67, 1–62, (2022).
- [8] R. Mutamimah, Susilo, and Y. Sardjono, "Aplikasi Program PHITS Versi 3.21 untuk Analisis Dosis Radiasi Pada Terapi Kanker Otak dengan Metode Proton Therapy" Unnes Phys. Educ. J., 11(1), 26–35, (2022).
- [9] I. Chambrelant, E. Jordan, A. Delphine, B. Héakuèdan, N. Georges, and A. Romane, "Proton Therapy and Gliomas: A Systematic Review" Radiation, 1(1), 218–233, (2021).
- [10] E. B. Podgoršak, Radiation Physics for Medical Physicists 2nd ed. Springer, (2010).
- [11] R. Wickert, T. Tessonnier, M. Deng, S. Adeberg, K. Seidensaal, L. Hoeltgen, J. Debus, K. Herfarth,

- and S. B. Harrabi, "Radiotherapy with Helium Ions Has the Potential to Improve Both Endocrine and Neurocognitive Outcome in Pediatric Patients with Ependymoma" Cancers, 14(23), 5865, (2022).
- [12] M. Vretenar, M. Angoletta, G. Bisoffi, J. Borburgh, L. Bottura, K. Palskis, R. Taylor, G. Tranquille, E. Benedetto, and M. Sapinski, "Conceptual Design of a Compact Synchroton-Based Facility For Cancer Therapy and Biomedical Research with Helium and Proton Beams" in Int. Part. Accel. Conf., 14, 5024–5027, (2023).
- [13] ICRP, "Recommendations of the International Commission on Radiological Protection" Ann. ICRP, 37(2–4), (2007).
- [14] S. Zarifi, H. T. Ahangari, S. B. Jia, M. A. Tajik-Mansoury, M. Najafzadeh, and M. P. Firouzjaei, "Bragg peak characteristics of proton beams within therapeutic energy range and the comparison of stopping power using the GATE Monte Carlo simulation and the NIST data" J. Radiothera. Pract., 19(2), 173–181, (2020).
- [15] Z. Alatas, S. Hidayati, Akhadi, M. Purba, D. Purwadi, S. Ariyanto, H. Winarno, Rismiyanto, E. Sofyatiningrum, W. Hendriyanto, H. Widyastono, E. M. Parmanto, and Syahril, "Buku Pintar Nuklir" Jakarta: BATAN, (2011).
- [16] I. D. A. Permatasari, "Analisis Berkas Radiasi Pesawat Radioterapi Linear Accelerator (LINAC) dengan Target Tungsten Menggunakan Software MCNPX" Universitas Sebelas Maret, Surakarta, (2018).
- [17] R. A. D. S. T. K. Wardani and Suharyana, "Analisis Distribusi Dosis Proton pada Terapi Proton untuk Kanker Glioblastoma menggunakan Software MCNP6" J. Fis., 13(1), 40–50, (2023).
- [18] M. A. Chanrion, F. Ammazzalorso, A. Wittig, R. E. Cabillic, and U. Jelen, "Dosimetric consequences of pencil beam width variations in scanned beam particle therapy" Phys. Med. Biol., 58, 3979–3993, (2013).
- [19] Y. Liu, Z. Li, R. Slopsema, and L. Hong, "TOPAS Monte Carlo simulation for double scattering proton therapy and dosimetric evaluation" Phys. Med., 62, 53–62, (2019).
- [20] A. Maharani, "Analisis Distribusi Dosis Terapi Proton dengan Kolimator Pencil Beam pada Kanker Glioblastoma menggunakan Software MCNP6" Universitas Sebelas Maret, Surakarta, (2022).